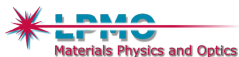


Control of optical properties of Ag-PVA plasmonic nanocomposites by film thickness: ellipsometry and multivariate analysis

Corentin Guyot and **Michel Voué**

University of Mons
Physics of Materials and Optics
Research Institute for Materials Science and Engineering
Mons - Belgium

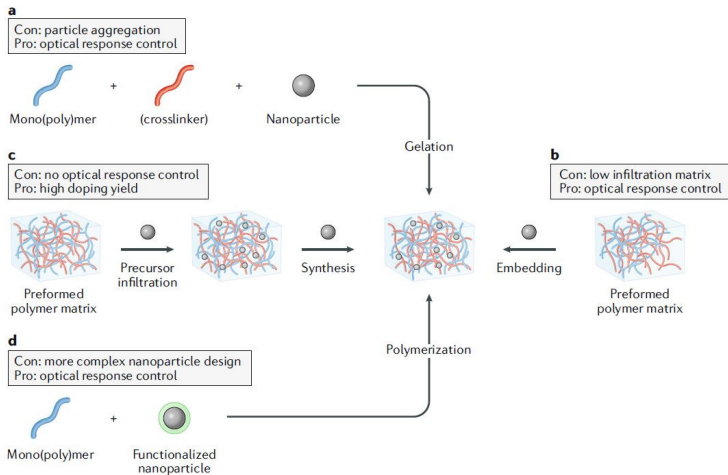
November 24, 2021



Publications

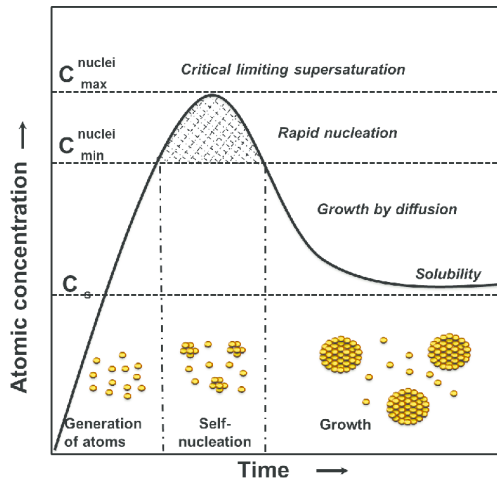
- ▶ Guyot Corentin, Voué Michel, "Intrinsic optical properties of Ag-doped poly-(vinyl alcohol) nanocomposites : an analysis of the film thickness effect on the plasmonic resonance parameters" in Applied Physics. A, Materials Science and Processing, 126, 870 (2020)
- ▶ Guyot Corentin, Leclère Philippe, Voué Michel, "Gold nanoparticles growing in a polymer matrix : what can we learn from spectroscopic imaging ellipsometry ?" in Journal of Vacuum Science and Technology. Part B, 38, 1, 013603 (2020)
- ▶ Guyot Corentin, Vandestruck Philippe, Marenne Ingrid, Deparis Olivier, Voué Michel, "Growth dynamics and light scattering of gold nanoparticles in situ synthesized at high concentration in thin polymer films" in Beilstein Journal of Nanotechnology, 10, 1768–1777 (2019)
- ▶ Guyot Corentin, "Plasmonic nanocomposites embedding gold and silver nanoparticles : in situ synthesis and local optical properties by spectroscopic imaging ellipsometry" , Voué Michel, 2012-09-17, Ph.D thesis, 2020-05-15 (2020)

Synthesis scheme



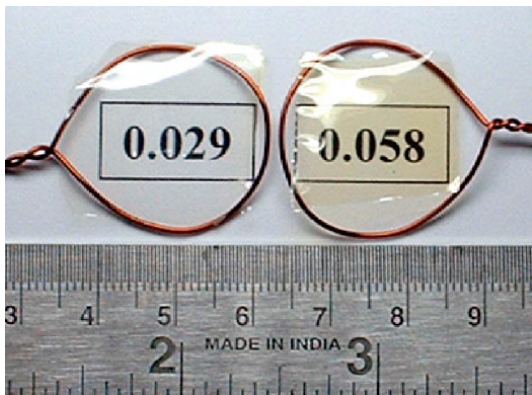
Pastoriza-Santos *et al*, Nature Reviews Materials (2018)
DOI : 10.1038/ s41578-018-0050-7

Lamer's diagram for colloidal solutions (1950)



Formation process of monodisperse particles.

C_0 : equilibrium concentration of solute with the bulk solid, $C_{nuclei\ min}$: critical concentration as the minimum concentration for nucleation, respectively. (I) prenucleation : generation of atoms, (II) self-nucleation, and (III) growth stages, respectively (Lamer and Dinegar, 1950).



Photographs of free-standing films of AgNPs in PVA matrix ; transparency of the films is demonstrated by placing them on wire frames above a paper on which the corresponding value of the Ag/PVA mass ratio is printed (Porel, 2007).

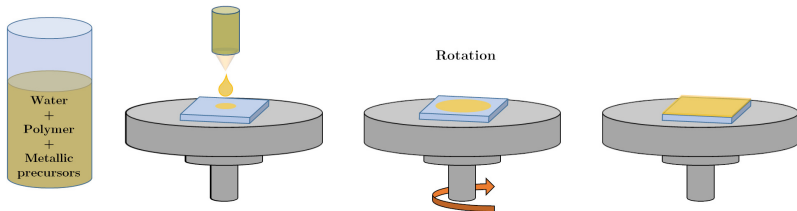
Some literature review for Silver-based PNCs

Articles	Nanocomposite reagents	Experimental processes	Optical methods	Main achievements
Khanna (2005)	AgNO ₃ , PVA and reducing agents	AgNPs formed in solution and casting, d : several micrometers	UV-visible spectrophotometry	Presence of AgNPs in thick PVA films
Nimrodh (2011)	AgNO ₃ , PVA and NaBH ₄	Casting, d : several micrometers, T : 50°C, t : 24 h	UV-visible spectrophotometry, SEM and DSC	AgNPs induce changes on the physical parameters of the PVA matrix
Karthikeyan (2005)	AgNO ₃ , PVA	Casting, d : several micrometers, T : 120°C, t : from 5 to 30 min	UV-visible spectrophotometry and FTIR	Increase of the absorbance as a function of the annealing time
Porel (2005, 2007, 2009a, 2009b)	AgNO ₃ , PVA or PVP	Spin coating, d : 3 - 6 μm or 500 - 600 nm, T : 110°C, t : from 5 to 60 min	UV-visible spectrophotometry, TEM and AFM	Blue-shift of λ _{LSPR} as a function of the annealing, spherical AgNPs
Oates (2006)	AgO ₂ , hfac, PS	Spin coating, d : 50 nm, T : from 120°C to 160°C, t : 30 min	SE, TEM and SEM	Determination of the size of the AgNPs using SE

Some literature review for Silver-based PNCs (2)

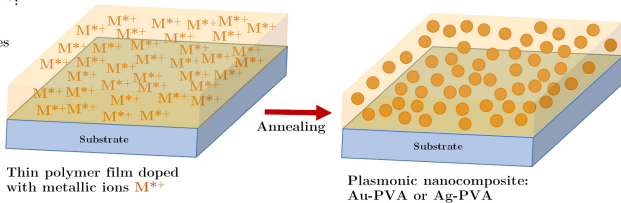
Articles	Nanocomposite reagents	Experimental processes	Optical methods	Main achievements
Clémenson (2006, 2007)	AgNO ₃ , PVA	Casting or spin coating, d : several micrometers or 150 nm, T : from 50 to 160°C, t : 60 min	UV-visible spectrophotometry, TEM	Variation of the annealing temperature, higher temperature larger AgNPs
Oates (2007)	AgNO ₃ , PVA	Spin coating, d : 90, 60 or 40 nm, T : from 120°C to 150°C, t : 60 min	SE and SEM	Following the growth of AgNPs with SE in real time
Voué (2008)	AgNO ₃ , PVA	Spin coating, d : 1 - 2 μm, T : 110°C, t : 60 min	FTIR-SE and AFM	Measurements in the IR region by FTIR-SE, bonds between Ag and PVA
Voué (2011)	AgNO ₃ , PVA	Spin coating, d : 1 - 2 and 0.6 - 0.7 μm, T : 90°C, t : from 5 to 60 min	SE and AFM	Determination of the optical properties of AgNPs in PVA matrix by SE
Guyot (2020)	AgNO ₃ , PVA	Spin-coating, d : 350 and 30 nm, T : 110°C, t : 60 min	Real time UV-visible spectrophotometry, AFM, SE and SIE	This presentation

Experimental protocol in more details ...



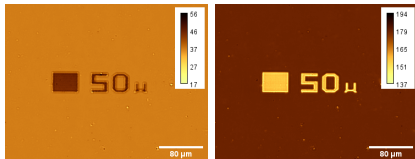
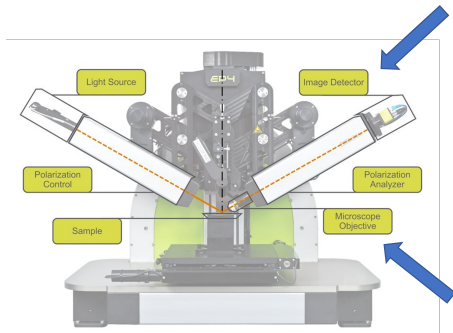
Metallic precursors M^{*+} :

- $\text{HAuCl}_4 \cdot 3\text{H}_2\text{O}$
for gold nanoparticles
- AgNO_3 for silver nanoparticles



Imaging Ellipsometry (IE)

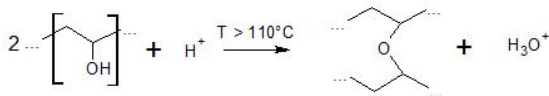
- ▶ combines **optical microscopy** and **ellipsometry** for spatially resolved layer-thickness and refractive index measurements of **micro-structured thin-films and substrates**.
- ▶ produces after optical modelling **images (maps)** of the measured quantities (thickness, refractive index, composition) at a spatial resolution of 1 $\mu\text{m}/\text{pixel}$



Ψ and Δ maps of a **100nm-thick SiO_2 pattern** on native oxide (Image at 658nm)

In situ reduction scheme of Ag^+

- ▶ Temperature for reduction : $T > 90^\circ\text{C}$
- ▶ Higher than the glass transition temperature of the polymer matrix ($T_g = 85^\circ\text{C}$)
- ▶ For $T > 110^\circ\text{C}$: crosslinking of the polymer matrix and less solubility to H_2O



(Top) Reduction scheme for the silver cations. (Bottom) Cross-linking of the PVA chains at high temperature (redrawn from Nicolais, 2014)

Optical properties of the polymer matrix

Polymer matrix only : spin coating of a 8% w :w PVA in water solution

- ▶ Film A to determine the optical properties, with spinning parameters : 2000 rpm during 90 s.
- ▶ Film B to confirm the optical properties, with spinning parameters : 6000 rpm during 90 s.



(A)

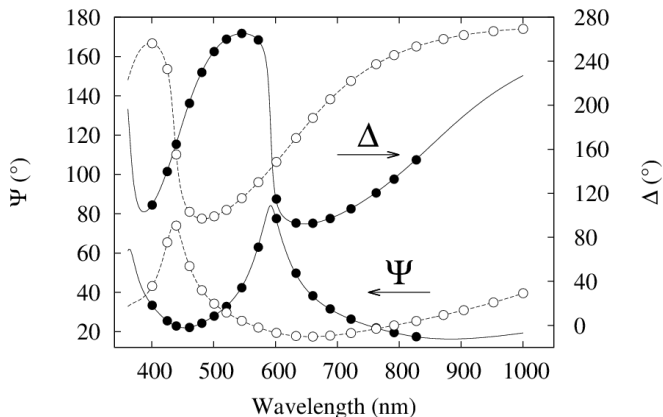


(B)



(A) PVA layer on silicon, (B) Cauchy model used to describe the optical properties of the PVA layer. Shaded area between the polymer layer and the substrate : SiO₂ layer.
(Not to scale)

Modeling of the optical properties



(Top curves) Δ (Bottom curves) Ψ . Closed symbols : 365 nm-thick film (optimisation of d and n). Open symbols : 266 nm-thick film (optimisation of d only). Plain and dashed lines : best-fit results.

Optimisation from SE data for PVA

Film A :

$$n_{\text{PVA}}(\lambda) = A_{\text{PVA}} + \frac{B_{\text{PVA}}}{\lambda^2} \quad \text{and} \quad k_{\text{PVA}}(\lambda) = 0$$

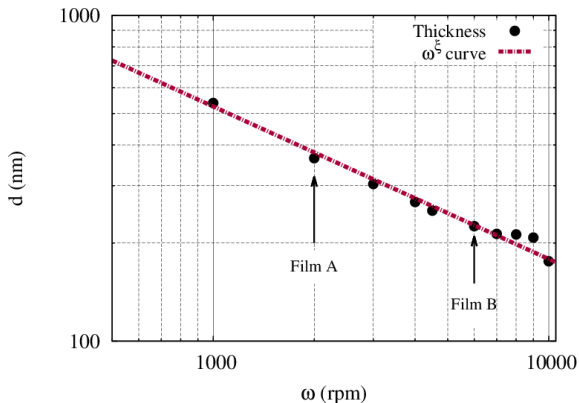
where A_{PVA} and B_{PVA} are the Cauchy coefficients.

$$A_n = 1.509 \pm 0.002 \quad \text{and} \quad B_n = 3172 \pm 296 \text{ nm}^2 \quad (\text{RMSE} = 0.966)$$

$$d_A = 365.2 \pm 0.6 \text{ nm}$$

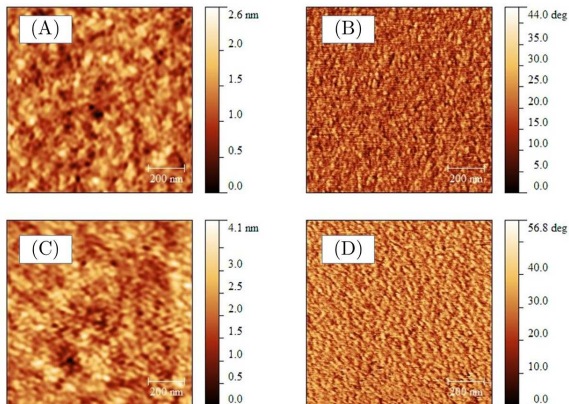
$$d_B = 266.1 \pm 0.1 \text{ nm} \quad (\text{RMSE} : 1.858)$$

Calibration curve for thin film coating



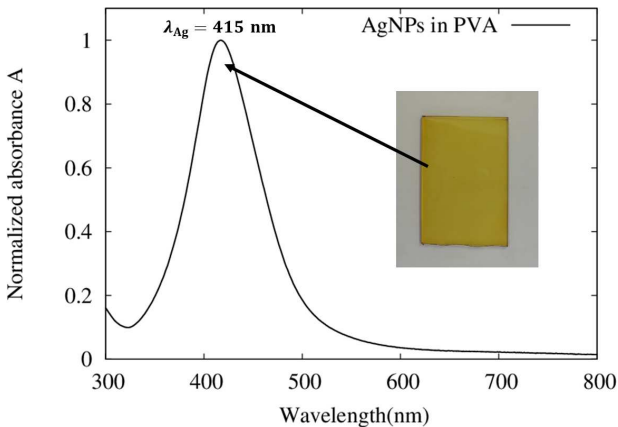
Calibration curve of the spin coater from undoped PVA solution in water (8% w :v).
Closed circles : experimental thickness (from SE). Red line : power law ω^ξ with
 $\xi = -0.468 \pm 0.017$ (Expected value : $\xi = -0.5$)

Topography of the PVA films by AFM



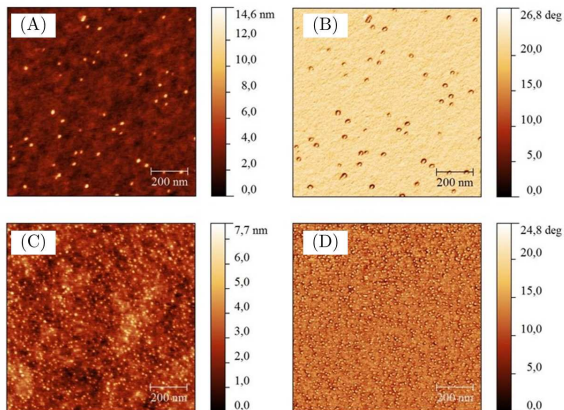
AFM topographic (left) and phase (right) images of the PVA control films. (A,B) 30 nm-thick films (C,D) 300 nm-thick films. Image size : $1 \mu\text{m} \times 1 \mu\text{m}$ (256×256 pixels).

UV-Vis spectra of AgPVA PNCs



Absorption spectrum of a glass coated with a thick film of AgNPs embedded in a PVA matrix at high doping level ($[Ag]/[PVA] = 25\% \text{ w : w}$). The inset picture is the analyzed sample.

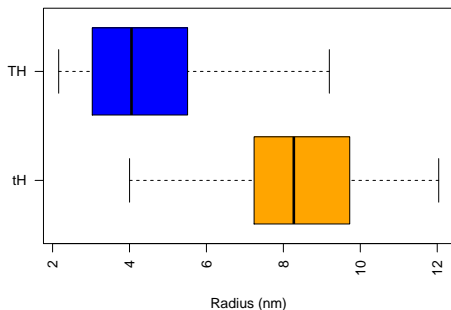
Topography of the Ag-PVA films



Topography (left) and phase (right) AFM images of Ag-PVA film doped with 25% AgNO_3 (w : w). (A, B) : $\simeq 30$ nm-thick film ; (C, D) : $\simeq 300$ nm-thick film. Image size : $1 \mu\text{m} \times 1 \mu\text{m}$ (256×256 pixels).

Film roughness and size of the particles

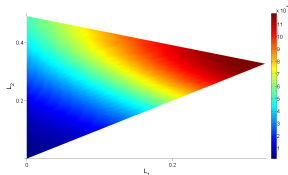
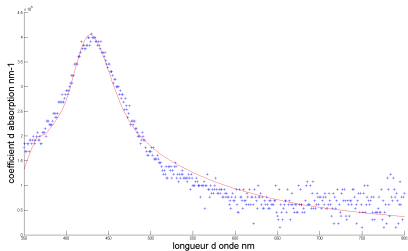
	Thick film		Thin film	
	Doped	Undoped	Doped	Undoped
S_a (nm)	0.66	0.40	0.59	0.32
S_q (nm)	0.85	0.52	0.77	0.42



Box-and-whiskers plots of the radius of the particles ([Ag]/[PVA] ratio : 25% ; film thickness : 30 nm ('th') and 300 nm ('TH')).

Depolarisation factor analysis

(Y. Battie, A. En Naciri, UDL)

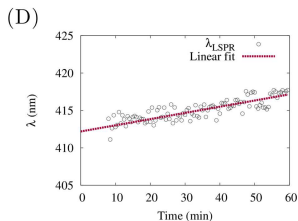
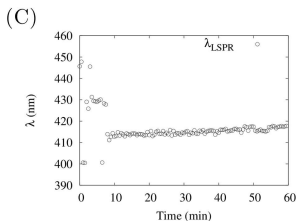
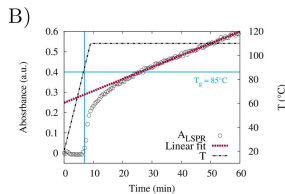
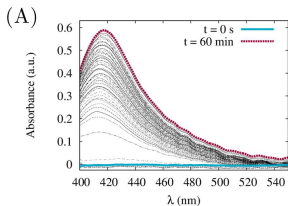


Ag-PVA film (8/2.5) – film thickness $\simeq 30$ nm : (Left) Modelling of the extinction spectra of a - (Right) Distribution of the depolarisation factors

Distribution centred around (1/3, 1/3, 1/3) : **Spherical NPs**

RT extinction spectroscopy of a Ag-PVA film

($d \sim 370$ nm)



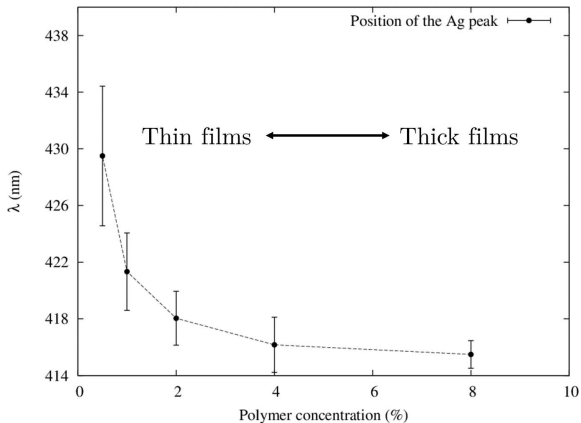
(A) Absorption spectra (B) Absorbance at λ_{SPR} [$A(t) \simeq 0.00585 t + 0.2481$]. (C) and (D) Resonance peak position as a function of time. $\lambda(t) = 0.083 t + 412.19$.

Film thickness effect at constant metal/polymer mass ratio

Samples ID	Polymer conc. (%)	Thickness (nm)	RMSE
[PVA] = 8%	8	374.9 ± 1.4	1.683
[PVA] = 4%	4	121.1 ± 0.1	0.709
[PVA] = 2%	2	54.5 ± 0.3	0.271
[PVA] = 1%	1	28.9 ± 0.1	0.205
[PVA] = 0.5%	0.5	15.8 ± 0.1	0.093

Measured thicknesses of the silver nanocomposite by the EP3-SE using Cauchy model. The model is applied on the ellipsometric data far from the resonance, i.e. for incident wavelength larger than 545 nm.

Red-shift of the resonance peak



Position of the resonance peak as a function of the polymer concentration.

Crossed effects of thickness and doping

The purpose of this analysis is two-fold :

- ▶ to compare **statistically** the optical properties of thick and thin films embedding AgNPs grown *in situ* from the same polymer solution ;
- ▶ to investigate the crossed effects of the doping of the film and of thicknesses.

Samples ID	Polymer conc. (%)	[Ag]/[PVA] mass ratio (%)	Coating speed (rpm)	Coating time (s)	Approx. thickness (nm)
TH	8	25	1600	60	300
TI	8	2.5	1600	60	300
tH	2	25	6000	60	30
tl	2	2.5	6000	60	30

Modelling of the optical properties

PVA layer : A one-layer Cauchy model is chosen to represent the optical properties of the PVA films in the transparent range

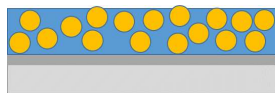
$$n_{\text{PVA}}(\lambda) = A_{\text{PVA}} + \frac{B_{\text{PVA}}}{\lambda^2} \quad \text{and} \quad k_{\text{PVA}}(\lambda) = 0$$

Ag-PVA layer : A Lorentzian oscillator is added to that model to account for the localized absorption of the plasmon resonance in visible range.

$$\varepsilon(\lambda) = \varepsilon_r(\lambda) + i\varepsilon_i(\lambda)$$
$$\varepsilon_r(\lambda) = \varepsilon_\infty + \frac{A\lambda^2(\lambda^2 - \Lambda_0^2)}{(\lambda^2 - \Lambda_0^2)^2 + \Gamma_0^2\lambda^2} \quad \varepsilon_i(\lambda) = \frac{A\lambda^3\Gamma_0}{(\lambda^2 - \Lambda_0^2)^2 + \Gamma_0^2\lambda^2}$$

(λ : wavelength, Λ_0 : resonance wavelength of the oscillator, A : oscillator strength, Γ_0 : full-width at half maximum (FWHM), ε_∞ : contributions of the resonances at wavelengths \gg than the measurable wavelength range.

Schematic representation of the optical model of Ag-PVA



(A)

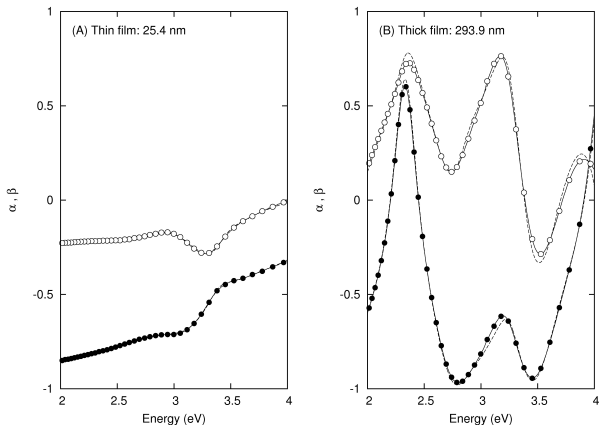


(B)



Schematic representation of the optical model used to interpret SE data : (A) AgNPs in PVA layer on Si and (B) a Cauchy model and Lorentzian oscillator used to describe the optical properties of AgNPs in PVA matrix. (Not to scale)

Ellipsometric spectra of Ag-doped PVA films



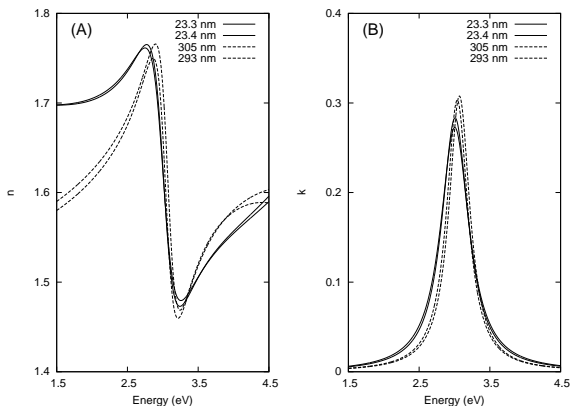
A, 'tH' thin films (thickness : 25.4 nm) ; B, 'TH' thick film (thickness : 293.9 nm).
Experimental data : $\alpha = \cos(2\Psi)$ (filled circles) and $\beta = \sin(2\Psi) \cos(\Delta)$ (open circles).
Dashed lines : optimized results from the optical model. ([Ag]/[PVA] ratio : 25% w :w)

Parameters of the plasmon absorption peak

Sample	d (nm)	A	Λ_0 (nm)	Γ_0 (nm)
Thin	23.4 ± 0.2	0.145 ± 0.006	414.2 ± 0.7	67.6 ± 2.9
	25.4 ± 0.3	0.133 ± 0.005	415.6 ± 0.6	69.0 ± 2.6
Thick	305.9 ± 1.7	0.117 ± 0.002	405.4 ± 0.7	47.3 ± 1.6
	293.4 ± 1.7	0.118 ± 0.002	409.5 ± 0.6	49.2 ± 1.5

Typical parameters of the plasmon absorption peak

Optical properties of thin and thick Ag-doped PVA films



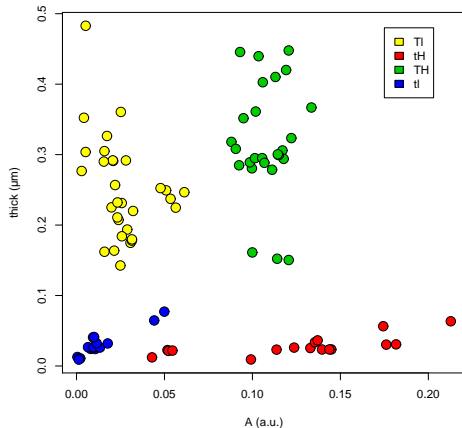
Optical properties of thin (plain lines) and thick (dashed lines) silver NPs-doped PVA films ([Ag]/[PVA] ratio : 25% w :w) : A, refractive index n ; B, extinction coefficient k .

Statistical distributions of the resonance parameters

class	N	thick	Means			Standard deviations			
			A	L0	Gamma	thick	A	L0	Gamma
tH	17	0.028	0.125	0.421	0.095	0.014	0.050	0.006	0.046
TH	27	0.311	0.102	0.410	0.064	0.082	0.018	0.005	0.018
tl	16	0.030	0.013	0.437	0.064	0.019	0.014	0.014	0.036
TI	30	0.254	0.028	0.419	0.127	0.076	0.024	0.013	0.056

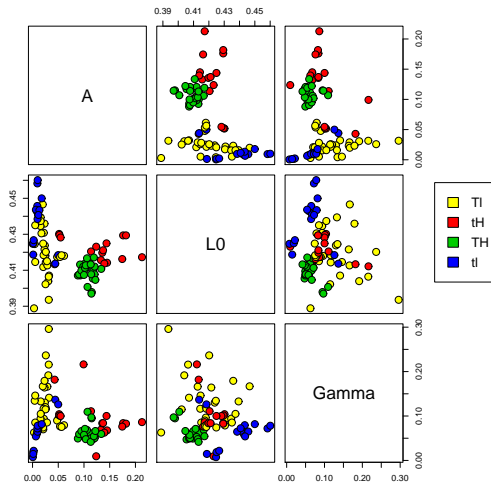
- ▶ Oscillator amplitude related to the doping level
- ▶ Less obvious for the other parameters *L0* and *Gamma*

Scatterplot



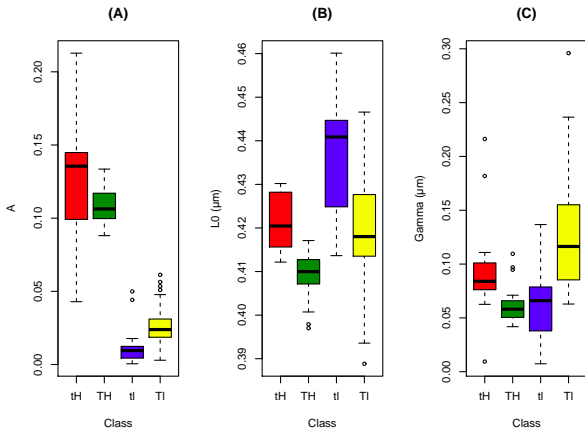
- ▶ Scatterplot of the thickness of the film (in μm) versus the strength of the oscillator.
- ▶ 4 separated sub-clouds

Scatterplot matrix



Scatterplot matrix of the resonance parameters. Units for peak position (“ $L0$ ” or Λ_0) and peak width (“ Γ ” or Γ_0) are micrometers.

Box-and-whiskers plots



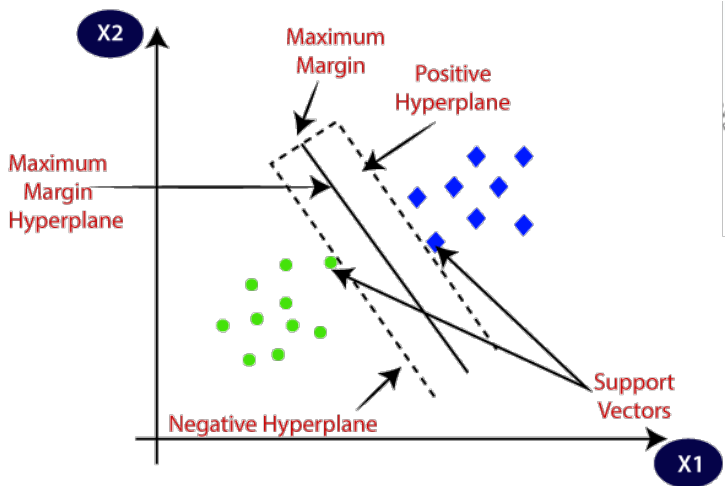
Box-and-whiskers plots of the resonance peaks parameters : (A) peak height (A), (B) peak position (L_0) and (C) peak width (Γ).

Statistical significance of the differences between classes

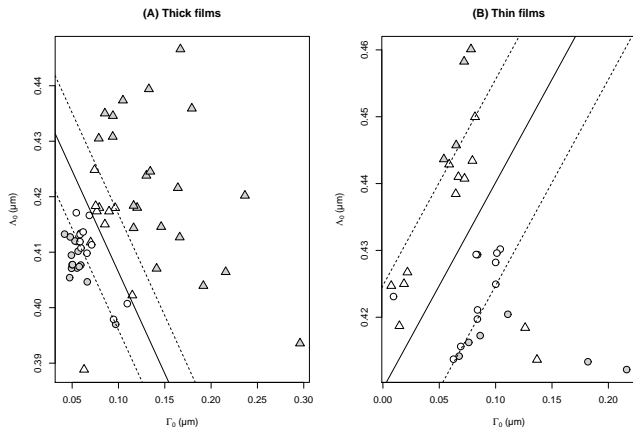
Parameter	Class			
	tH	TH	tl	TI
A	a	a	b	c
Λ_0	b	c	a	b
Γ_0	b	c	c	a

- ▶ No equality of the variances
- ▶ **Kruskal-Wallis** statistical tests with *posthoc* comparison tests
- ▶ Classes represented by the same letter do not statistically differ from each other.

Support Vector Machines (SVM)(Vapnik, 1995)

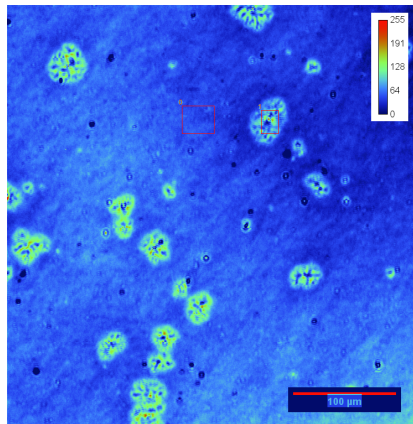


Classification in the $\Lambda_0 - \Gamma$ plane



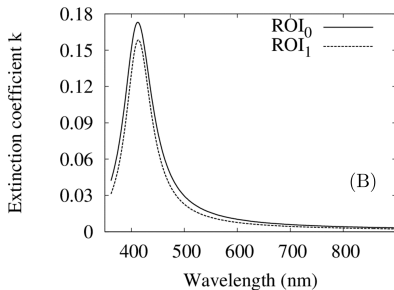
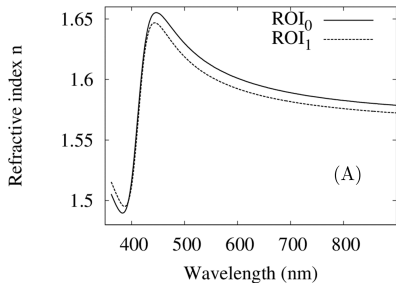
(A) Thick films (B) Thin films ([Ag]/[PVA] ratio : 25% (circles) and 2.5% (triangles) ;
Open symbols : support vectors ; Lines : optimum classifier (plain) and margin
(dashed).

Ellipsometric enhanced contrast (EEC) images at high silver concentration



Ellipsometric enhanced contrast (grey levels, in false color) image of the Ag–PVA film at the end of the annealing (Scalebar : 100 μm , wavelength : 545 nm, AOI : 42°). Red rectangles indicates the regions of interest "0" and "1" used for spectroscopic characterization.

Local optical properties



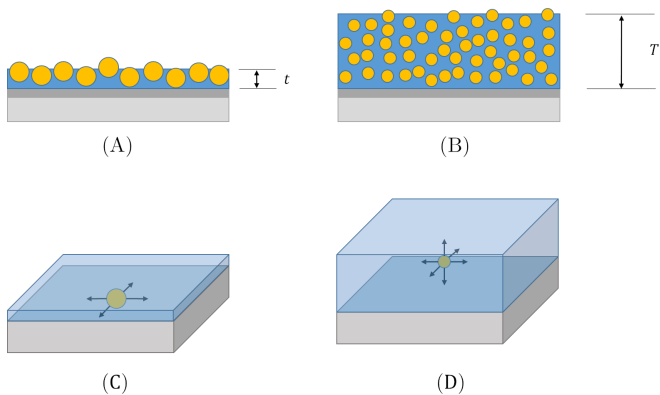
Optical properties of 445.7 nm-thick silver nanocomposite film ([Ag] : [PVA] ratio : 25% w : w) : A, refractive index n ; B, extinction coefficient k .

SIE local fits for Ag-PVA films

Table 1 – Best-fit results of the ellipsometric data obtained with the SIE on AgNPs embedded in PVA matrix within the Lorentzian term in order to take into account the absorption peak.

ROI	Thickness (nm)	Amplitude (eV ²)	Frequency (eV)	Damping (eV)	RMSE
0	445.7 ± 3.0	0.786 ± 0.021	3.000 ± 0.014	0.480 ± 0.021	3.179
1	445.2 ± 3.3	0.608 ± 0.021	2.979 ± 0.012	0.378 ± 0.027	3.405

Scheme of the NPs growth



Conclusions, prospects and open questions

- ▶ Influence of the film thickness on the intrinsic optical properties
- ▶ Red shift of the resonance band for thin films at constant metal/polymer mass ratio
- ▶ Spherical nanoparticles
- ▶ No influence of the polymer mass (pure diffusion) at constant thickness

- ▶ "Real" distribution of the NPs in thin films by AFM, SEM or TEM
- ▶ Diffusion/aggregation model via molecular dynamics or Monte-Carlo methods
- ▶ Extension to NPs with other particle shapes
- ▶ Multilayered PNCs as model for hyperbolic metamaterials

Acknowledgements

- ▶ Dr. Corentin Guyot (B-Sens Technology, Mons)
- ▶ Dr. Gilles Rosolen, Pr. Philippe Leclère (UMONS)
- ▶ Dr. Peter Thiesen & Dr. Mathias Duwe (Accurion GmbH, Gottingen)
- ▶ FRS-FNRS
- ▶ UMONS – Research Institute for Materials Science and Engineering



Thank you for your attention